LETTER

doi:10.1038/nature10261

Sideband cooling of micromechanical motion to the quantum ground state

J. D. Teufel[1], T. Donner[2,3], Dale Li[1], J. W. Harlow[2,3], M. S. Allman[1,3], K. Cicak[1], A. J. Sirois[1,3], J. D. Whittaker[1,3], K. W. Lehnert[2,3] & R. W. Simmonds[1]

The advent of laser cooling techniques revolutionized the study of many atomic-scale systems, fuelling progress towards quantum computing with trapped ions[1] and generating new states of matter with Bose–Einstein condensates[2]. Analogous cooling techniques[3,4] can provide a general and flexible method of preparing macroscopic objects in their motional ground state. Cavity optomechanical or electromechanical systems achieve sideband cooling through the strong interaction between light and motion[5–15]. However, entering the quantum regime—in which a system has less than a single quantum of motion—has been difficult because sideband cooling has not sufficiently overwhelmed the coupling of low-frequency mechanical systems to their hot environments. Here we demonstrate sideband cooling of an approximately 10-MHz micromechanical oscillator to the quantum ground state. This achievement required a large electromechanical interaction, which was obtained by embedding a micromechanical membrane into a superconducting microwave resonant circuit. To verify the cooling of the membrane motion to a phonon occupation of 0.34 ± 0.05 phonons, we perform a near-Heisenberg-limited position measurement[3] within $(5.1 \pm 0.4)\hbar/2\pi$, where $\hbar$ is Planck's constant. Furthermore, our device exhibits strong coupling, allowing coherent exchange of microwave photons and mechanical phonons[16]. Simultaneously achieving strong coupling, ground state preparation and efficient measurement sets the stage for rapid advances in the control and detection of non-classical states of motion[17,18], possibly even testing quantum theory itself in the unexplored region of larger size and mass[19]. Because mechanical oscillators can couple to light of any frequency, they could also serve as a unique intermediary for transferring quantum information between microwave and optical domains[20].

A mechanical oscillator of high quality factor placed within the quantum regime could allow us to explore quantum mechanics in entirely new ways[17–20]. To do this requires the ability to prepare the oscillator in its ground state, to arbitrarily control its quantum states, and to detect these states near the Heisenberg limit. In addition, the oscillator system should not be strongly perturbed by its environment or any other extraneous influence, including dissipation or thermal excitations. As a first step, the oscillator's temperature T must be reduced so that $k_B T < \hbar\Omega_m$, where Ω_m is the resonance frequency of the oscillator, k_B is Boltzmann's constant, and $\hbar$ is $h/2\pi$. Although there has been substantial progress in cooling mechanical oscillators with radiation pressure forces, sideband cooling to the quantum mechanical ground state has been a long-standing challenge. Cavity optomechanical systems have realized very large sideband cooling rates[9–13,15]; however, these rates are not sufficient to overcome the larger thermal heating rates of the mechanical modes. Electromechanical experiments using much lower-energy microwave photons[5–8,14], although simpler to operate below 100 mK, have suffered from weak electromechanical interactions and inefficient detection of the photon fields.

In a unique approach, a system based on a high-frequency (6-GHz) microwave dilatation oscillator was integrated with a superconducting phase qubit[21]. Its high frequency offered the advantage of reaching the ground state at relatively high temperatures ($T \approx 25$ mK), which were achievable simply with passive dilution refrigeration. Furthermore, because the mechanical oscillator was piezoelectric, its strong electrical response enabled significantly strong coupling to the superconducting qubit, providing direct control and (destructive) measurement of the phonon energy states. These results showed that quantum effects are achievable with a human-fabricated mechanical oscillator. Unfortunately, the short mechanical lifetimes prevented the manipulation of complex mechanical states and direct tests of entanglement.

Low frequency (<100-MHz) mechanical oscillators have distinct advantages: higher quality factors, long phonon lifetimes and large motional state displacements, which are important for future tests of quantum theory[19]. Cavity opto- or electro-mechanical systems[4] naturally offer a powerful method for both cooling and detecting low-frequency mechanical oscillators[22,23]. An object whose motion alters the resonance frequency, ω_c, of an electromagnetic cavity experiences a radiation pressure force governed by the parametric interaction Hamiltonian: $\hat{H}_{int} = \hbar G \hat{n} \hat{x}$, where $G = d\omega_c/dx$, $\hat{n}$ is the cavity photon number, and $\hat{x}$ is the displacement of the mechanical oscillator. By driving the cavity at a frequency ω_d, the oscillator's motion produces upper and lower sidebands at $\omega_d \pm \Omega_m$. Because these sideband photons are inelastically scattered from the drive field, they provide a way to exchange energy with the oscillator. If the drive field is optimally detuned below the cavity resonance by an amount $\Delta \equiv \omega_d - \omega_c = -\Omega_m$, photons will be preferentially up-converted to ω_c because the photon density of states is maximal there (Fig. 1b). When an up-converted photon leaves the cavity, it removes the energy of one mechanical quantum (one phonon) from the motion. Thus, the mechanical oscillator is damped and cooled by way of this radiation-pressure force. Because the mechanical motion is encoded in the scattered photons leaving the cavity, information on the position of the mechanical oscillator provides a near Heisenberg-limited measurement of displacement[24].

Here we use a cavity electromechanical system where a flexural mode of a thin aluminium membrane is parametrically coupled to a superconducting microwave resonant circuit. Unlike previous microwave systems, this device achieves large electromechanical coupling by use of a flexible vacuum-gap capacitor[16,25]. The oscillator is a 100-nm-thick aluminium membrane with a diameter of 15 μm, suspended 50 nm above a second aluminium layer on a sapphire substrate[25] (Fig. 1). These two metal layers form a parallel-plate capacitor that is shunted by a 12-nH spiral inductor. This combination of capacitor and inductor creates a microwave cavity with a displacement-dependent resonance frequency centred at $\omega_c = 2\pi \times 7.54$ GHz. The device is operated in a dilution refrigerator at 15 mK, at which temperature aluminium is superconducting, and the microwave cavity has a total energy decay rate of $\kappa \approx 2\pi \times 200$ kHz. The diameter of the aluminium membrane and its tension[8] produce an Ω_m of $2\pi \times 10.56$ MHz with an intrinsic damping rate of $\Gamma_m = 2\pi \times 32$ Hz, or mechanical quality factor $Q_m = \Omega_m/\Gamma_m = 3.3 \times 10^5$. The oscillator mass, $m = 48$ pg, implies that

[1]National Institute of Standards and Technology (NIST), Boulder, Colorado 80305, USA. [2]JILA, University of Colorado and NIST, Boulder, Colorado 80309, USA. [3]Department of Physics, University of Colorado, Boulder, Colorado 80309, USA.

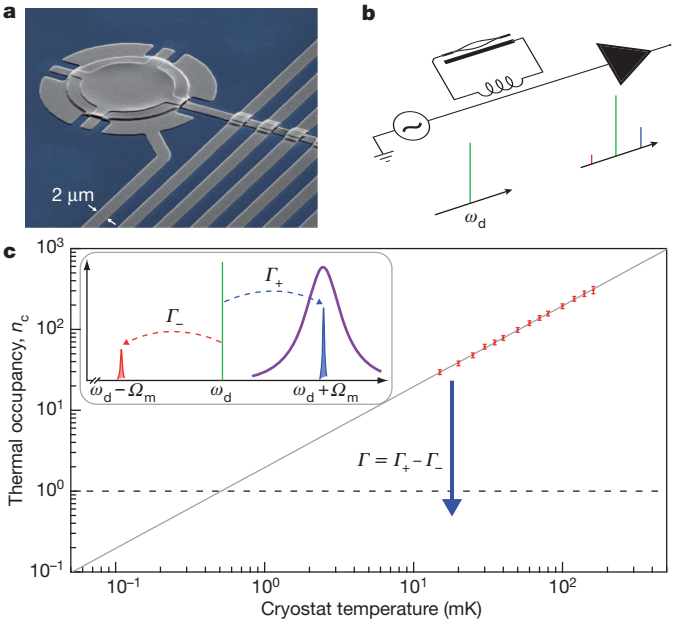

Figure 1 | Schematic description of the experiment. **a**, False-colour scanning electron micrograph showing the aluminium (grey) electromechanical circuit fabricated on a sapphire (blue) substrate; a 15-μm-diameter membrane is suspended 50 nm above a lower electrode. The membrane's motion modulates the capacitance, and hence, the resonance frequency of the superconducting microwave circuit. **b**, A coherent microwave drive (left, ω_d, shown green in frequency–amplitude plot below) inductively coupled to the circuit (top) acquires modulation sidebands (red and blue in plot below) owing to the thermal motion of the membrane. The upper sideband is amplified with a nearly quantum-limited Josephson parametric amplifier (filled triangle, right) within the cryostat. **c**, The microwave power in the upper sideband provides a direct measurement of the thermal occupancy of the mechanical mode, which may be calibrated *in situ* by varying the temperature of the cryostat (main panel). The mechanical mode shows thermalization with the cryostat at all temperatures, yielding a minimum thermal occupancy of 30 mechanical quanta without using sideband-cooling techniques. Error bars, s.d. Inset, illustration of the concept of sideband cooling. When the circuit is excited with a detuned microwave drive such that $\Delta = -\Omega_m$, the narrow line shape of the electrical resonance ensures that the rate to scatter photons to higher energy Γ_+ (blue dashed arrow, blue peak) exceeds the rate to scatter to lower energy Γ_- (red dashed arrow, red peak). Thus, the net scattering rate Γ (blue solid arrow) provides a cooling mechanism for the membrane.

the zero-point motion is $x_{zp} = \sqrt{\hbar/(2m\Omega_m)} = 4.1$ fm. With a ratio of $\Omega_m/\kappa > 50$, our system is deep within the resolved-sideband regime and well-suited for sideband cooling to the mechanical ground state[22,23].

To measure the mechanical displacement, we apply a microwave field, which is detuned below the cavity resonance frequency by $\Delta = -\Omega_m$, through heavily attenuated coaxial lines to the feed line of our device. The upper sideband, now at ω_c, is amplified with a custom-built Josephson parametric amplifier[26,27] followed by a low-noise cryogenic amplifier, demodulated at room temperature, and finally monitored with a spectrum analyser. The thermal motion of the membrane creates an easily resolvable peak in the microwave noise spectrum. As described previously[27], this measurement scheme constitutes a nearly shot-noise-limited microwave interferometer with which we can measure mechanical displacement with minimum added noise close to fundamental limits.

In order to calibrate the demodulated signal to the membrane's motion, we measure the thermal noise spectrum while varying the cryostat temperature (Fig. 1c). Here a weak microwave drive (~3 photons in the cavity) is used in order to ensure that radiation pressure damping and cooling effects are negligible. When $\Omega_m \gg \kappa \gg \Gamma_m$ and $\Delta = -\Omega_m$, the displacement spectral density S_x is related to the observed microwave noise spectral density S by $S_x = 2(\kappa\Omega_m/G\kappa_{ex})^2 S/P_o$, where κ_{ex} is the coupling rate between the cavity and the feed line, and P_o is the power of the microwave drive at the output of the cavity. According to equipartition, the area under the resonance curve of displacement spectral density S_x must be proportional to the effective temperature of the mechanical mode. This calibration procedure allows us to convert the sideband in the microwave power spectral density to a displacement spectral density and to extract the thermal occupation of the mechanical mode. In Fig. 1c we show the number of thermal quanta in the mechanical resonator as a function of T. The linear dependence of the integrated power spectral density with temperature shows that the mechanical mode equilibrates with the cryostat even for the lowest achievable temperature of 15 mK. This temperature corresponds to a thermal occupancy $n_m = 30$, where $n_m = [\exp(\hbar\Omega_m/k_BT) - 1]^{-1}$. The calibration determines the electromechanical coupling strength, $G/2\pi = 49 \pm 2$ MHz nm^{-1}. With these device parameters, we can investigate both the fundamental sensitivity of our measurement and the effects of radiation pressure cooling.

The total measured displacement noise results from two sources: the membrane's actual mean-square motion, S_x^{th}, and its apparent motion, S_x^{imp}, which is due to imprecision of the measurement. Figure 2a demonstrates how the use of low-noise parametric amplification significantly

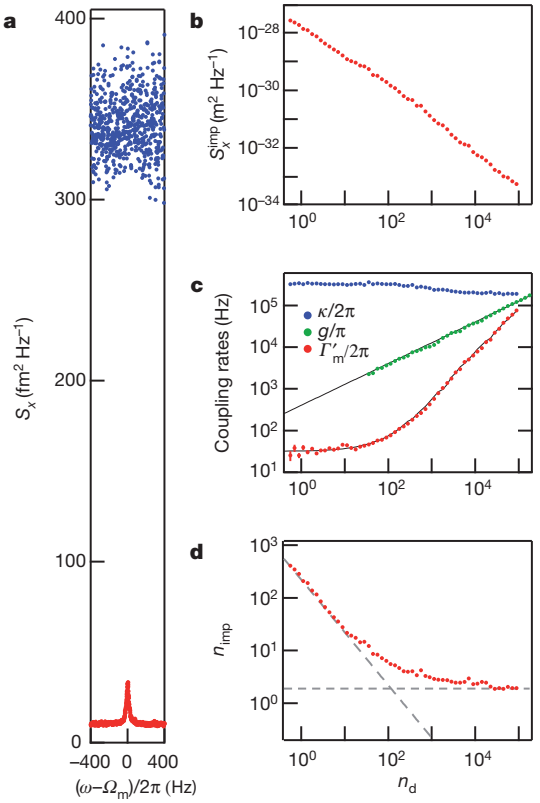

Figure 2 | Displacement sensitivity in the presence of dynamical back-action. **a**, The displacement spectral density S_x measured with (red) and without (blue) the Josephson parametric amplifier. As the parametric amplifier greatly reduces the total noise of the microwave measurement, the time required to resolve the thermal motion is reduced by a factor of 1,000. **b**, As the microwave drive power is increased, the absolute displacement sensitivity, S_x^{imp} improves, reaching a minimum of 5.5×10^{-34} m^2 Hz^{-1} at the highest power. **c**, The parametric coupling rate g between the microwave cavity and the mechanical mode increases as $\sqrt{n_d}$. This coupling broadens the linewidth of the mechanical mode Γ'_m from its intrinsic value of $\Gamma_m = 2\pi \times 32$ Hz until it exceeds the linewidth of the microwave cavity κ. **d**, The relative measurement imprecision, in units of mechanical quanta, depends on the product of S_x^{imp} and Γ'_m. Thus, once the power is large enough that dynamical back-action overwhelms the intrinsic mechanical linewidth, n_{imp} asymptotically approaches a constant value ($n_{imp} = 1.9$), which is a direct measure of the overall efficiency of the photon measurement.

lowers S_x^{imp}, resulting in a reduction in the white-noise background by a factor of more than 30. This greatly increases the signal-to-noise ratio of the membrane's thermal motion, thereby reducing the integration time required to resolve the thermal peak by a factor of 1,000. To investigate the measurement sensitivity in the presence of dynamical back-action, we regulate the cryostat temperature at 20 mK and increase the amplitude of the detuned microwave drive while observing modifications in the displacement spectral density. We quantify the strength of the drive by the resulting number of photons n_d in the microwave cavity. As shown in Fig. 2b, the measurement imprecision S_x^{imp} is inversely proportional to n_d. At the highest drive power ($n_d \approx 10^5$), the absolute displacement sensitivity is $5.5 \times 10^{-34}\,m^2\,Hz^{-1}$.

As expected, the increased drive power also damps and cools the mechanical oscillator[3,22,23]. The total mechanical dissipation rate $\Gamma'_m = \Gamma_m + \Gamma$ is the sum of the intrinsic dissipation, Γ_m, and the radiation-pressure-induced damping resulting from scattering photons to the upper/lower sideband, $\Gamma = \Gamma_+ - \Gamma_-$, where $\Gamma_\pm = 4g^2\kappa/[\kappa^2 + 4(\Delta \pm \Omega_m)^2]$. Here g is the coupling rate between the cavity and the mechanical mode, which depends on the amplitude of the drive: $g = Gx_{zp}\sqrt{n_d}$. Figure 2c shows the measured values of κ, g and Γ'_m as the drive increases. The radiation-pressure damping of the mechanical oscillator becomes pronounced above a cavity drive amplitude of approximately 75 photons, at which point $\Gamma'_m = 2\Gamma_m$ and the mechanical linewidth has doubled. Note that the increased damping rate can be switched off at any time by removing the cooling drive, returning the mechanical oscillator to its intrinsic quality factor, Q_m.

Whereas the absolute value of the displacement imprecision decreases with increasing power, the visibility of the thermal mechanical peak no longer improves once the radiation-pressure force becomes the dominant dissipation mechanism for the membrane. By expressing the imprecision as equivalent thermal quanta of the oscillator, $n_{imp} = \Gamma'_m S_x^{imp}/8x_{zp}^2$, we see that the visibility of the thermal noise above the imprecision no longer improves once the drive is much greater than $n_d \approx 100$ (Fig. 2d). This is because a linear decrease in S_x^{imp} is balanced by a linear increase in Γ'_m due to radiation-pressure damping. The asymptotic value of n_{imp} is a direct measure of the efficiency of the microwave measurement. Ideally, for a lossless circuit, a quantum-limited microwave measurement would imply $n_{imp} = 1/4$. The incorporation of the low-noise Josephson parametric amplifier improves n_{imp} close to this ideal limit, reducing the asymptotic value of n_{imp} from 70 to 1.9 quanta. This level of sensitivity is crucial for resolving any residual thermal motion when cooling into the quantum regime.

Beginning from a cryostat temperature of 20 mK and a thermal occupation of $n_m^T = 40$ quanta, the fundamental mechanical mode of the membrane is cooled by radiation-pressure forces. Figure 3a shows the displacement spectral density of the motional sideband as n_d is increased from 18 to 4,500 photons, along with fits to a Lorentzian lineshape (shaded areas). As described above, this increased drive results in three effects on the spectra: lower noise floor, wider resonances and smaller shaded area. Because the shaded area corresponds to the mean-square membrane displacement, it directly measures the effective temperature of the mode. At a drive intensity with 4,000

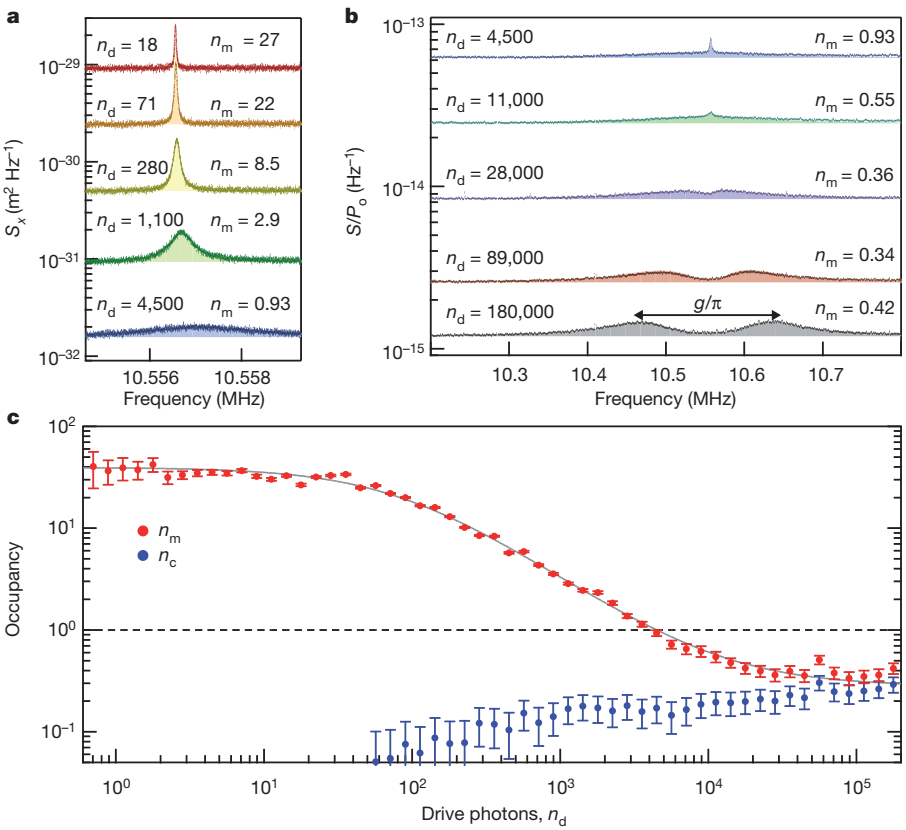

Figure 3 | Sideband cooling the mechanical mode to the ground state. a, The displacement noise spectra and Lorentzian fits (shaded regions) for five different drive powers. With higher power, the mechanical mode is both damped (larger linewidth) and cooled (smaller area) by the radiation pressure forces. **b**, Over a broader frequency span, the normalized sideband noise spectra clearly show both the narrow mechanical peak and a broader cavity peak due to finite occupancy of the mechanical and electrical modes, respectively. A small, but resolvable, thermal population of the cavity appears as the drive power increases, setting the limit for the final occupancy of the coupled optomechanical system. At the highest drive power, the coupling rate between the mechanical oscillator and the microwave cavity exceeds the intrinsic dissipation of either mode, and the system hybridizes into optomechanical normal modes. **c**, Starting in thermal equilibrium with the cryostat at $T = 20$ mK, sideband cooling reduces the thermal occupancy of the mechanical mode from $n_m = 40$ into the quantum regime, reaching a minimum of $n_m = 0.34 \pm 0.05$. Error bars, s.d. These data demonstrate that the parametric interaction between photons and phonons can initialize the strongly coupled, electromechanical system in its quantum ground state.

photons in the cavity, the thermal occupation is reduced below one quantum of mechanical motion, entering the quantum regime.

Observing the noise spectrum over a broader frequency range reveals that in addition to the mechanical Lorentzian peak with linewidth Γ'_{m}, there is also a Lorentzian peak with linewidth κ whose area corresponds to the finite thermal occupation n_{c} of the cavity. Over this range, it is no longer valid to evaluate the cavity parameters at a single frequency to infer the spectrum in units of S_x. Instead, Fig. 3b shows the noise spectrum in units of sideband power normalized by the power at the drive frequency, S/P_{o}. These two sources of noise, originating from either the mechanical or the electrical mode, interfere with each other and result in noise squashing[14] and eventually normal-mode splitting[28] once $2g > \kappa/\sqrt{2}$. Using a quantum-mechanical description applied to our circuit[14,24], the expected noise spectrum as a function of frequency ω is:

$$S = \hbar\omega\left(\frac{1}{2} + n_{\mathrm{add}} + 2\kappa_{\mathrm{ex}}\frac{\kappa n_{\mathrm{c}}\left(\Gamma_{\mathrm{m}}^2 + 4\delta^2\right) + 4\Gamma_{\mathrm{m}} n_{\mathrm{m}}^T g^2}{\left|4g^2 + \left(\kappa + 2j\left(\delta + \tilde{\Delta}\right)\right)\left(\Gamma_{\mathrm{m}} + 2j\delta\right)\right|^2}\right) \qquad (1)$$

where $j = \sqrt{-1}$, $\delta = \omega - \Omega_{\mathrm{m}}$, $\tilde{\Delta} = \omega_{\mathrm{d}} + \Omega_{\mathrm{m}} - \omega_{\mathrm{c}}$, and n_{add} is added noise of the microwave measurement expressed as an equivalent number of microwave photons. Figure 3b shows the measured spectra and corresponding fits (shaded regions) to equation (1) as the electromechanical system evolves first into the quantum regime ($n_{\mathrm{m}}, n_{\mathrm{c}} < 1$) and then into the strong-coupling regime ($2g > \kappa/2$). The results are summarized in Fig. 3c, where the thermal occupancy of both the mechanical and electrical modes is shown as a function of n_{d}. For low drive power, the cavity shows no resolvable thermal population (to within our measurement uncertainty of 0.05 quanta), as expected for a 7.5-GHz mode at 20 mK. Although it is unclear whether the observed population at higher drive power is a consequence of direct heating of the substrate, heating of the microwave attenuators preceding the circuit, or intrinsic cavity frequency noise, we have determined that it is not the result of frequency or amplitude noise of our microwave generator, as this noise is reduced far below the microwave shot-noise level with narrow-band filtering and cryogenic attenuation (see Supplementary Information). Sideband cooling can never reduce the occupancy of the mechanical mode below that of the cavity. Therefore, in order for the system to access the quantum regime, the thermal population of the cavity must remain less than one quantum. Assuming $\Omega_{\mathrm{m}} \gg \kappa$, the final occupancy of a mechanical mode is[28]:

$$n_{\mathrm{m}} = n_{\mathrm{m}}^T\left(\frac{\Gamma_{\mathrm{m}}}{\kappa}\frac{4g^2 + \kappa^2}{4g^2 + \kappa\Gamma_{\mathrm{m}}}\right) + n_{\mathrm{c}}\left(\frac{4g^2}{4g^2 + \kappa\Gamma_{\mathrm{m}}}\right) \qquad (2)$$

This equation shows that for moderate coupling ($\sqrt{\kappa\Gamma_{\mathrm{m}}} \ll g \ll \kappa$) the cooling of the mechanical mode is linear in the number of drive photons. Beyond this regime, the onset of normal-mode splitting abates further cooling. Here the mechanical cooling rate becomes limited not by the coupling between the mechanical mode and the cavity, but instead by the coupling rate κ between the cavity and its environment[28]. Thus, the final occupancy of the mechanical mode can never be reduced to lower than $n_{\mathrm{m}}^T\Gamma_{\mathrm{m}}/\kappa$, and a stronger parametric drive will only increase the Rabi frequency at which the thermal excitations oscillate between the cavity and mechanical modes. For our device, as the coupling is increased, we first cool to the ground state and then enter the strong-coupling regime ($n_{\mathrm{m}}^T\Gamma_{\mathrm{m}} < \kappa < g$). Once n_{d} exceeds 2×10^4, the mechanical occupancy converges towards the cavity population, reaching a minimum of 0.34 ± 0.05 quanta. At the highest power drive ($n_{\mathrm{d}} = 2 \times 10^5$), the mechanical mode has hybridized with the cavity, resulting in the normal-mode splitting characteristic of the strong-coupling regime[16,29]. This level of coupling is required to use the hybrid system for quantum information processing. The strong-coupling regime ensures that quantum states of this combined system may be manipulated faster than they decohere from spurious interaction with either electromagnetic or mechanical environments.

Taken together, the measurements shown in Figs 2 and 3 quantify the overall measurement efficiency of the system. The Heisenberg limit requires that a continuous displacement measurement is necessarily accompanied by a back-action force[3,13,24], such that $\sqrt{S_x^{\mathrm{imp}} S_F^{\mathrm{ba}}} \geq \hbar$, where S_F^{ba} is the force noise spectral density from back-action alone. From the thermal occupancy and damping rate of the mechanical mode, we extract a total force spectral density $S_F^{\mathrm{tot}} = 4\hbar\Omega_{\mathrm{m}} m\Gamma'_{\mathrm{m}}(n_{\mathrm{m}} + 1/2)$. By attributing all of S_F^{tot} to back-action, we can place a conservative upper bound on the imprecision-back-action product with $\sqrt{S_x^{\mathrm{imp}} S_F^{\mathrm{tot}}}/\hbar = \sqrt{n_{\mathrm{imp}}(n_{\mathrm{m}} + 1/2)} \leq 5.1 \pm 0.4$. The minimum achievable value with our detuned probe tone (see Supplementary Information) is $\sqrt{S_x^{\mathrm{imp}} S_F^{\mathrm{ba}}} = \hbar\sqrt{2}$, making this experiment a factor of 3.6 away from the Heisenberg-limit for displacement detection, the narrowest gap achieved to date[15,24].

Looking forward, this technology offers a feasible route to achieve many of the long-standing goals for mechanical quantum systems. Whereas the resolved-sideband regime is well-suited for efficient sideband cooling, it makes a simultaneous measurement of both the upper and lower sideband difficult. By simply increasing the bandwidth of the cavity, future experiments could feasibly measure the zero-point motion of the mechanical mode, as well as observe the fundamental asymmetry between the rates of emission and absorption of phonons[1]. Other prospects include quantum non-demolition measurements[3] and the generation of entangled states of mechanical motion[17,18]. Furthermore, combining this device with a superconducting qubit[21] would allow for the direct measurement of the mechanical oscillator's energy states and the preparation of arbitrary quantum states of mechanical motion[30]. Because the interaction between the 10.6-MHz mechanical mode and the 7.5-GHz microwave cavity is parametric, the coupling strength is inherently tunable, and can be turned on and off quickly. Thus, once a quantum state is transferred into the mechanical mode, it can be stored there for a time $\tau_{\mathrm{th}} = 1/\left(n_{\mathrm{m}}^T\Gamma_{\mathrm{m}}\right) > 100\ \mu\mathrm{s}$ before absorbing one thermal phonon from its environment. As this timescale is much longer than typical coherence times of superconducting qubits, mechanical modes offer the potential for delay and storage of quantum information. Lastly, mechanical objects provide a generic system for interacting with a wide range of different physical systems—ranging from magnetic spins to optical photons—leading towards future methods for engineering the coherent transfer of quantum information between vastly different forms of quanta[20].

The power and versatility of sideband cooling techniques have now been used to bring a high quality, macroscopic ($\sim 10^{12}$ atoms) low-frequency mechanical oscillator into the quantum regime. This electromechanical system simultaneously demonstrates ground-state preparation, strong-coupling and near quantum-limited position detection, paving the way to accessing the quantum nature of long-lived motional states.

Received 22 February; accepted 2 June 2011.
Published online 6 July 2011.

1. Diedrich, F., Bergquist, J. C., Itano, W. M. & Wineland, D. J. Laser cooling to the zero-point energy of motion. *Phys. Rev. Lett.* **62,** 403–406 (1989).
2. Anderson, M. H., Ensher, J. R., Matthews, M. R., Wieman, C. E. & Cornell, E. A. Observation of Bose-Einstein condensation in a dilute atomic vapor. *Science* **269,** 198–201 (1995).
3. Braginsky, V. B. & Khalili, F. Y. *Quantum Measurement* (Cambridge Univ. Press, 1992).
4. Kippenberg, T. J. & Vahala, K. J. Cavity optomechanics: back-action at the mesoscale. *Science* **321,** 1172–1176 (2008).
5. Braginsky, V. B., Manukin, A. B. & Tikhonov, M. Y. Investigation of dissipative ponderomotive effects of electromagnetic radiation. *Sov. Phys. JETP* **31,** 829–830 (1970).
6. Blair, D. G. *et al.* High sensitivity gravitational wave antenna with parametric transducer readout. *Phys. Rev. Lett.* **74,** 1908–1911 (1995).
7. Cuthbertson, B. D., Tobar, M. E., Ivanov, E. N. & Blair, D. G. Parametric back-action effects in a high-Q cryogenic sapphire transducer. *Rev. Sci. Instrum.* **67,** 2435–2442 (1996).
8. Teufel, J. D., Harlow, J. W., Regal, C. A. & Lehnert, K. W. Dynamical backaction of microwave fields on a nanomechanical oscillator. *Phys. Rev. Lett.* **101,** 197203 (2008).

9. Thompson, J. D. *et al.* Strong dispersive coupling of a high-finesse cavity to a micromechanical membrane. *Nature* **452,** 72–75 (2008).
10. Gröblacher, S. *et al.* Demonstration of an ultracold micro-optomechanical oscillator in a cryogenic cavity. *Nature Phys.* **5,** 485–488 (2009).
11. Park, Y.-S. & Wang, H. Resolved-sideband and cryogenic cooling of an optomechanical resonator. *Nature Phys.* **5,** 489–493 (2009).
12. Lin, Q., Rosenberg, J., Jiang, X., Vahala, K. J. & Painter, O. Mechanical oscillation and cooling actuated by the optical gradient force. *Phys. Rev. Lett.* **103,** 103601 (2009).
13. Schliesser, A., Arcizet, O., Rivière, R., Anetsberger, G. & Kippenberg, T. J. Resolved-sideband cooling and position measurement of a micromechanical oscillator close to the Heisenberg uncertainty limit. *Nature Phys.* **5,** 509–514 (2009).
14. Rocheleau, T. *et al.* Preparation and detection of a mechanical resonator near the ground state of motion. *Nature* **463,** 72–75 (2010).
15. Rivière, R. *et al.* Optomechanical sideband cooling of a micromechanical oscillator close to the quantum ground state. Preprint at ⟨http://arXiv.org/abs/1011.0290⟩ (2010).
16. Teufel, J. D. *et al.* Circuit cavity electromechanics in the strong coupling regime. *Nature* **471,** 204–208 (2011).
17. Bose, S., Jacobs, K. & Knight, P. L. Preparation of nonclassical states in cavities with a moving mirror. *Phys. Rev. A* **56,** 4175–4186 (1997).
18. Mancini, S., Man'ko, V. I. & Tombesi, P. Ponderomotive control of quantum macroscopic coherence. *Phys. Rev. A* **55,** 3042–3050 (1997).
19. Marshall, W., Simon, C., Penrose, R. & Bouwmeester, D. Towards quantum superpositions of a mirror. *Phys. Rev. Lett.* **91,** 130401 (2003).
20. Regal, C. A. & Lehnert, K. W. From cavity electromechanics to cavity optomechanics. *J. Phys. Conf. Ser.* **264,** 012025 (2011).
21. O'Connell, A. D. *et al.* Quantum ground state and single-phonon control of a mechanical resonator. *Nature* **464,** 697–703 (2010).
22. Marquardt, F., Chen, J. P., Clerk, A. A. & Girvin, S. M. Quantum theory of cavity-assisted sideband cooling of mechanical motion. *Phys. Rev. Lett.* **99,** 093902 (2007).
23. Wilson-Rae, I., Nooshi, N., Zwerger, W. & Kippenberg, T. J. Theory of ground state cooling of a mechanical oscillator using dynamical backaction. *Phys. Rev. Lett.* **99,** 093901 (2007).
24. Clerk, A. A., Devoret, M. H., Girvin, S. M., Marquardt, F. & Schoelkopf, R. J. Introduction to quantum noise, measurement, and amplification. *Rev. Mod. Phys.* **82,** 1155–1208 (2010).
25. Cicak, K. *et al.* Low-loss superconducting resonant circuits using vacuum-gap-based microwave components. *Appl. Phys. Lett.* **96,** 093502 (2010).
26. Castellanos-Beltran, M. A., Irwin, K. D., Hilton, G. C., Vale, L. R. & Lehnert, K. W. Amplification and squeezing of quantum noise with a tunable Josephson metamaterial. *Nature Phys.* **4,** 929–931 (2008).
27. Teufel, J. D., Donner, T., Castellanos-Beltran, M. A., Harlow, J. W. & Lehnert, K. W. Nanomechanical motion measured with an imprecision below that at the standard quantum limit. *Nature Nanotechnol.* **4,** 820–823 (2009).
28. Dobrindt, J. M., Wilson-Rae, I. & Kippenberg, T. J. Parametric normal-mode splitting in cavity optomechanics. *Phys. Rev. Lett.* **101,** 263602 (2008).
29. Gröblacher, S., Hammerer, K., Vanner, M. R. & Aspelmeyer, M. Observation of strong coupling between a micromechanical resonator and an optical cavity field. *Nature* **460,** 724–727 (2009).
30. Hofheinz, M. *et al.* Synthesizing arbitrary quantum states in a superconducting resonator. *Nature* **459,** 546–549 (2009).

Supplementary Information is linked to the online version of the paper at www.nature.com/nature.

Acknowledgements We thank A. W. Sanders for taking the micrograph in Fig. 1 and the JILA instrument shop for fabrication and design of the cavity filter. This work was supported by NIST and the DARPA QuASAR programme. T.D. acknowledges support from the Deutsche Forschungsgemeinschft (DFG). This Letter is a contribution of the US government and not subject to copyright.

Author Contributions J.D.T. and R.W.S. conceived the device. J.D.T. designed the circuit. J.D.T. and D.L. fabricated the devices. J.D.T. and T.D. set up the experiment, performed the measurements and analysed the data. J.D.T., T.D., R.W.S. and K.W.L. discussed the results and wrote the manuscript. All authors provided experimental support and commented on the manuscript.

Author Information Reprints and permissions information is available at www.nature.com/reprints. The authors declare no competing financial interests. Readers are welcome to comment on the online version of this article at www.nature.com/nature. Correspondence and requests for materials should be addressed to J.D.T. (john.teufel@nist.gov).